Cell

# Single Naive CD4$^+$ T Cells from a Diverse Repertoire Produce Different Effector Cell Types during Infection

Noah J. Tubo,[1] Antonio J. Pagán,[1] Justin J. Taylor,[1] Ryan W. Nelson,[1] Jonathan L. Linehan,[1] James M. Ertelt,[2] Eric S. Huseby,[3] Sing Sing Way,[2] and Marc K. Jenkins[1,*]
[1]Department of Microbiology, Center for Immunology
[2]Department of Pediatrics, Center for Infectious Disease and Microbiology/Translational Research
University of Minnesota Medical School, Minneapolis, MN 55455, USA
[3]Department of Pathology, University of Massachusetts Medical School, Worcester, MA 01655, USA
*Correspondence: jenki002@umn.edu
http://dx.doi.org/10.1016/j.cell.2013.04.007

## SUMMARY

A naive CD4$^+$ T cell population specific for a microbial peptide:major histocompatibility complex II ligand (p:MHCII) typically consists of about 100 cells, each with a different T cell receptor (TCR). Following infection, this population produces a consistent ratio of effector cells that activate microbicidal functions of macrophages or help B cells make antibodies. We studied the mechanism that underlies this division of labor by tracking the progeny of single naive T cells. Different naive cells produced distinct ratios of macrophage and B cell helpers but yielded the characteristic ratio when averaged together. The effector cell pattern produced by a given naive cell correlated with the TCR-p:MHCII dwell time or the amount of p:MHCII. Thus, the consistent production of effector cell subsets by a polyclonal population of naive cells results from averaging the diverse behaviors of individual clones, which are instructed in part by the strength of TCR signaling.

## INTRODUCTION

Each newly formed naive CD4$^+$ T cell expresses a unique T cell antigen receptor (TCR) with the potential to bind to a specific foreign peptide bound to a host major histocompatibility complex II (MHCII) molecule (Davis et al., 1998; Marrack et al., 2008). During infection, microbes are carried to secondary lymphoid organs, where antigen-presenting cells (APC) degrade microbial proteins into peptides, some of which bind an MHCII molecule and are displayed on the APC surface (Itano and Jenkins, 2003). About one in a million naive CD4$^+$ T cells will by chance express a TCR with specificity for one of these peptide:MHCII complexes (p:MHCII) (Jenkins et al., 2010). Interaction with an APC displaying the relevant p:MHCII will cause the TCR on a naive T cell to transduce signals leading to proliferation (Smith-Garvin et al., 2009).

The proliferating T cells then differentiate into effector cells that enhance the microbicidal activities of macrophages or help B cells secrete antibodies (Zhu et al., 2010). This process has been studied during acute infections with an attenuated strain of the *Listeria monocytogenes* (Lm) bacterium or lymphocytic choriomeningitis virus (LCMV) (Marshall et al., 2011; Pepper et al., 2011). Early after infection, naive CD4$^+$ T cells with microbe p:MHCII-specific TCRs proliferate and differentiate into Th1 effector cells, which produce the macrophage-activating cytokine IFN-$\gamma$, or into one of two types of follicular helper cells—Tfh cells that augment B cell activation at the border between the T cell areas and follicles or GC-Tfh cells that drive affinity maturation in germinal centers (Choi et al., 2011; Crotty, 2011; Lee et al., 2011; Pepper et al., 2011). Tfh and GC-Tfh cells express CXCR5, a chemokine receptor that directs cell migration to the follicles and germinal centers (Ansel et al., 1999) but differ by increased PD-1 expression on GC-Tfh (Crotty, 2011). Although most of these effector cells die as the infection is cleared, some survive as memory cells (Pepper and Jenkins, 2011).

Effector cell differentiation is controlled by the IL-2 receptor and the Bcl-6 transcription factor. IL-2 receptor signaling promotes the Th1 fate (Pepper et al., 2011) by stimulating production of the Blimp1 transcription factor, which suppresses Bcl-6 needed for Tfh and GC-Tfh differentiation (Johnston et al., 2012), and the IL-12 receptor (Liao et al., 2011), which promotes T-bet expression by activating STAT4. The Tfh and GC-Tfh fates are reinforced in cells lacking IL-2 receptor by signals through inducible T cell costimulator (ICOS) (Choi et al., 2011; Johnston et al., 2009; Nurieva et al., 2008). In this model, the TCR is a switch that makes the T cell receptive to external inputs by inducing the IL-2 receptor, IL-12 receptor, or ICOS. Some studies, however, indicate that the strength of the TCR signal itself influences the quality of effector cell differentiation (Bretscher et al., 1992; Constant et al., 1995; Deenick et al., 2010; Fazilleau et al., 2009; Hosken et al., 1995; Parish and Liew, 1972).

If differentiation patterns are determined only by environmental factors, such as cytokines, then naive cells with different TCRs should produce similar effector cell types in the same

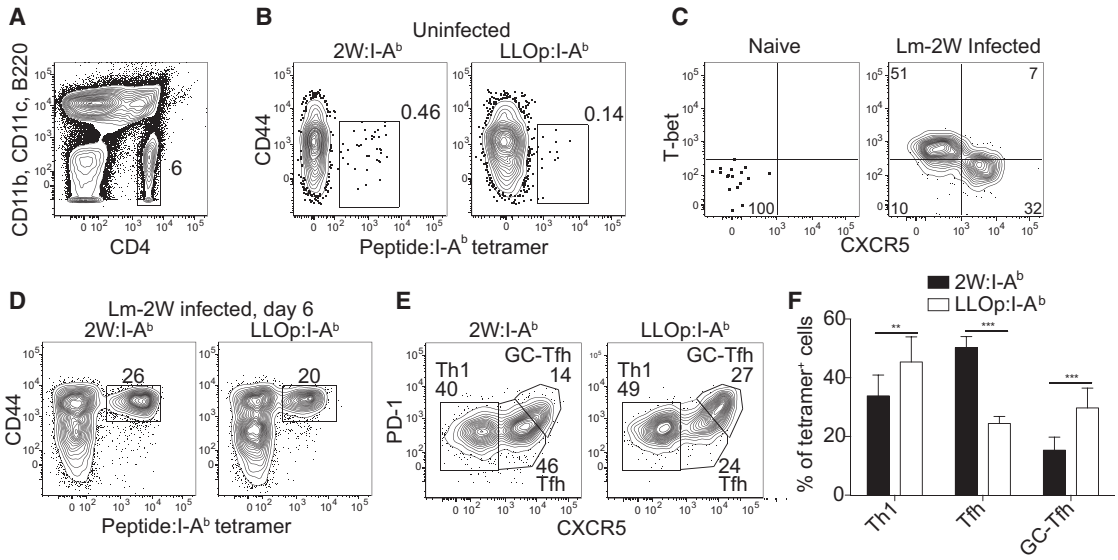


**Figure 1. LLOp:I-A$^b$- and 2W:I-A$^b$-Specific Effector Cells Have Consistent Patterns of Differentiation after Lm Infection**

(A) Plot showing identification of CD4$^+$ T cells from the bound fraction after enrichment with p:I-A$^b$ tetramer.

(B) CD4$^+$ T cells identified as in (A) from a naive B6 mouse with a gate on CD44$^{low}$ 2W:I-A$^{b+}$ (left) or LLOp:I-A$^{b+}$ (right) cells.

(C) Plots of T-bet and CXCR5 for LLOp:I-A$^b$-specific cells from a naive B6 mouse (left) or a B6 mouse 7 days after Lm infection (right).

(D) CD4$^+$ T cells identified as in (A) from a B6 mouse 6 days after Lm-2W infection with a gate on CD44$^{high}$ 2W:I-A$^{b+}$ (left) or LLOp:I-A$^{b+}$ (right) cells.

(E) Plots used to identify CXCR5$^-$ PD-1$^-$ Th1, CXCR5$^{int}$ PD-1$^-$ Tfh, and CXCR5$^{high}$ PD-1$^+$ GC-Tfh cells among 2W:I-A$^b$-specific (left) and LLOp:I-A$^b$-specific (right) cells identified as in (D), 6 days after Lm infection.

(F) Percentage ± SD (n = 10) of 2W:I-A$^{b+}$ (black bars) and LLOp:I-A$^{b+}$ (white bars) CD4$^+$ T cells that were Th1, Tfh, or GC-Tfh cells, 6 days after Lm infection.

infection. However, if differentiation is instructed by the TCR-p:MHCII interaction, then naive cells with different TCRs would not necessarily differentiate equivalently. We explored this issue here by tracking the progeny of single naive CD4$^+$ T cells during infection. Our results lead to the conclusion that each naive T cell has a tendency to produce certain types of effector cells, in part because of the nature of its unique TCR.

## RESULTS

### Naive T Cells Specific for Unique p:MHCII Undergo Distinct Patterns of Differentiation

Lm infection of C57BL/6 (B6) mice was used to assess the CD4$^+$ T cell response to different p:MHCII during the same infection. An attenuated Lm strain was engineered to secrete chicken ovalbumin fused to the 2W variant of MHCII I-E$\alpha_{52\text{-}68}$ (Ertelt et al., 2009), a known immunogenic peptide that binds to the I-A$^b$ MHCII molecule of B6 mice (Rees et al., 1999). These bacteria also express listeriolysin O (LLO) (Portnoy et al., 2002), which contains the I-A$^b$-binding peptide LLO$_{190\text{-}201}$ (LLOp) (Geginat et al., 2001). Phagocytes in the spleen and lymph nodes (LN) quickly clear these bacteria after infection (Portnoy et al., 2002) and, in the process, produce I-A$^b$ molecules loaded with bacterial peptides. These complexes are then presented to small populations of naive T cells, which proliferate and differentiate into Th1, Tfh, or GC-Tfh effector cells (Moon et al., 2007; Pepper et al., 2011).

A sensitive flow-cytometry-based cell enrichment method (Moon et al., 2007) was used to determine whether LLOp:I-A$^b$- and 2W:I-A$^b$-specific T cells had similar patterns of differentiation. Spleen and LN cells from individual B6 mice were mixed with fluorochrome-conjugated LLOp:I-A$^b$ or 2W:I-A$^b$ tetramers and magnetic beads and then passed over magnetized columns. The cells that bound to the columns were then stained with antibodies specific for informative cell-surface molecules and analyzed by flow cytometry. In all cases, the bound cells contained CD4$^+$ T cells, although the majority of the cells were non-T cells (Figure 1A). About 200 2W:I-A$^b$ tetramer-binding and 50 LLOp:I-A$^b$ tetramer-binding cells were detected in the CD4$^+$ population (Figure 1B) from uninfected mice. LLOp:I-A$^b$ or 2W:I-A$^b$ tetramer-binding cells were not detected among the CD8$^+$ cells in the bound fraction (data not shown; Moon et al., 2007; Pepper et al., 2011), indicating that tetramer binding was TCR specific. Tetramer-binding CD4$^+$ T cells from uninfected mice expressed low amounts of CD44 (Figure 1B) and did not express T-bet or CXCR5 (Figure 1C) as expected for naive cells (Jenkins et al., 2010).

By 1 week after intravenous infection with Lm-2W bacteria, the 2W:I-A$^b$- and LLOp:I-A$^b$-specific naive T cells produced many CD44$^{high}$ effector cells (Figure 1D), some T-bet$^{high}$ CXCR5$^-$ and some T-bet$^{low}$ CXCR5$^+$ (data not shown; Figure 1C). Analysis of CXCR5 and PD-1 revealed that the two epitope-specific populations produced different effector cell patterns. The 2W:I-A$^b$-specific population consisted of about 40% Th1 (CXCR5$^-$), 50% Tfh (CXCR5$^+$ PD-1$^-$), and 10% GC-Tfh (CXCR5$^+$ PD-1$^+$) cells, whereas the LLOp:I-A$^b$-specific population consisted of about 50% Th1, 25% Tfh, and 25% GC-Tfh cells (Figures 1E and 1F). Thus, effector cells specific for these two epitopes

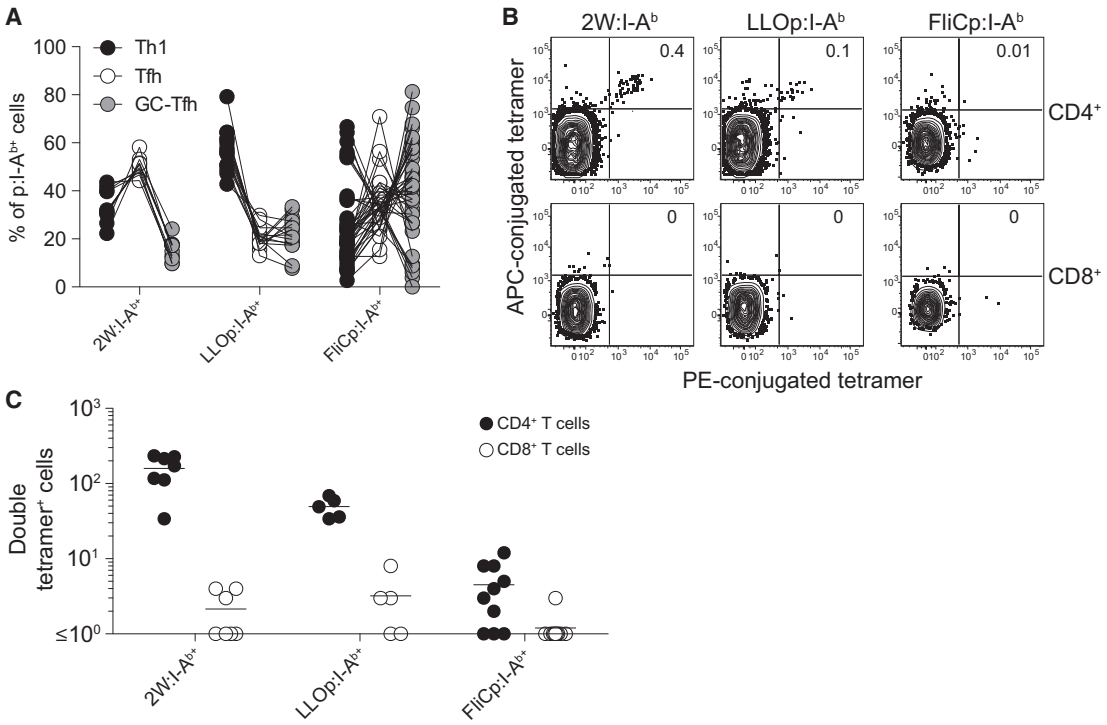


**Figure 2. A Small Naive CD4$^+$ T Population Produces Variable Effector Cell Patterns in Individual Mice**

(A) Percentages of CD4$^+$ T cells specific for 2W:I-A$^b$, LLOp:I-A$^b$, or FliCp:I-A$^b$ that were Th1 (black circles), Tfh (white circles), or GC-Tfh (gray circles) cells in B6 mice, 6 to 7 days after infection with Lm bacteria expressing the relevant peptide. Lines connect values for the same mouse.

(B) Plots of tetramer staining for CD4$^+$ (top row) or CD8$^+$ T cells (bottom row) from spleen and LN of individual naive B6 mice following enrichment with the indicated peptide:I-A$^b$ tetramers labeled with two different fluorochromes.

(C) Number of double tetramer-binding CD4$^+$ (black circles) or CD8$^+$ T cells (white circles) found in individual mice identified as shown in (B).

exhibited different patterns of differentiation when generated in the same environment.

Analysis of the *Salmonella typhimurium* FliC$_{427\text{-}441}$ (FliCp):I-A$^b$ epitope yielded another pattern of effector cell differentiation. In this case, the percentages of Th1, Tfh, and GC-Tfh effector cells from individual mice were plotted to assess the mouse-to-mouse variability of the response (Figure 2A). This presentation underscored the finding that the 2W:I-A$^b$- and LLOp:I-A$^b$-specific effector cells generated by Lm-2W infection had different patterns but were consistent among different mice. In contrast, the FliCp:I-A$^b$-specific effector cells generated by Lm-FliC infection showed dramatic mouse-to-mouse variability.

It was possible that this variability was related to the small size of the FliCp:I-A$^b$-specific naive cell population, which we previously estimated to consist of about 20 cells per mouse (Moon et al., 2007). This issue was revisited here with a modified cell enrichment method designed to eliminate the few cells that bound tetramer nonspecifically. Cells were stained with a mixture of the same p:MHCII tetramer labeled with either phycoerythrin or allophycocyanin, with the assumption that cells with a p:MHCII-specific TCR would bind to both tetramers (Stetson et al., 2002). A small number of CD4$^+$, but not CD8$^+$ T, cells from uninfected B6 mice bound to FliCp:I-A$^b$, LLOp:I-A$^b$, or 2W:I-A$^b$ tetramers with both fluorochromes (Figure 2B). Importantly, double tetramer staining excluded the cells that bound to only one of the tetramers in a non-TCR-specific fashion (Figure 2B). Taking into account only double tetramer-stained CD4$^+$ T cells, uninfected B6 mice contained on average 160 2W:I-A$^b$-, 50 LLOp:I-A$^b$-, and 4 FliCp:I-A$^b$-specific naive cells (Figure 2C). Thus, the repertoire of FliCp:I-A$^b$-specific naive cells was at least an order of magnitude smaller than those specific for the other epitopes and produced effector cell populations of variable composition in different individual mice. Together, the results indicate that the TCR must instruct effector cell differentiation because the only qualitative difference between the LLOp:I-A$^b$-, 2W:I-A$^b$-, and FliC:I-A$^b$-specific naive populations is their TCR specificity.

## Different Naive T Cells from a Polyclonal Repertoire Produce Distinct Types of Effector Cells

Because each cell in a naive p:MHCII-specific population expresses a different TCR (Moon et al., 2011), it was possible that the unique TCR on each naive cell signals differently to produce a certain effector cell differentiation pattern. A limiting dilution approach was used to test this possibility. CD4$^+$ T cells from CD45.1$^+$, CD90.1$^+$, or CD45.1$^+$ CD45.2$^+$ mice were transferred into B6 mice in numbers expected to contain on average less than one LLOp:I-A$^b$-specific naive CD4$^+$ T cell. These mice were then infected with Lm bacteria, and recipient and donor

LLOp:I-A$^b$-specific cells were identified with CD45.1, CD90.1, and CD45.2 antibodies 6 to 7 days later.

B6 mice that did not receive donor T cells contained many LLOp:I-A$^b$-specific effector cells 1 week after Lm infection, of which less than two stained nonspecifically with CD45.1, CD90.1, or CD45.1 and CD45.2 antibodies (Figure 3A). This low background allowed unambiguous detection of donor-derived effector cell populations (Figures 3B and 3C). Of 34 recipients, 5 contained CD45.1$^+$, 11 contained CD90.1$^+$, 4 contained CD45.1$^+$ CD45.2$^+$ donor-derived cells, and a few recipients contained two different donor cell-derived populations. Based on these values and the Poisson distribution (Taswell, 1981), there was a high probability that these 20 donor-derived populations were the progeny of single naive cells.

The genes encoding the TCR Vβ-Jβ-Dβ segments (*Tcrb-VDJ*) were sequenced from single cells to confirm this contention. As expected, ten randomly selected CD4$^+$ T cells from a B6 mouse each had a different *Tcrb-VDJ* sequence with a unique complementarity-determining region 3 (CDR3) (Table 1). Sequences were also obtained for 22 single cells isolated from polyclonal LLOp:I-A$^b$-specific cells from a B6 mouse 7 days after Lm infection. Four sequences were found in more than one cell, and *Tcrb-V14* was found in 12 cells, indicating the presence of immunodominant clones in the LLOp:I-A$^b$-specific population. Finally, we obtained sequences for 7–18 single cells from four different donor-derived LLOp:I-A$^b$-specific populations in four different Lm-infected recipients of limiting numbers of donor T cells. Each of the four populations had a different *Tcrb-VDJ* sequence with a unique CDR3. Importantly, all of the single cells from a given donor-derived population had the identical *Tcrb-VDJ* sequence. These results demonstrate that donor-derived LLOp:I-A$^b$-specific cells in recipients of limiting numbers of donor T cells were the progeny of single naive cells.

The phenotypic heterogeneity of the clonal donor populations was then assessed. Effector cell populations generated from the 20 single LLOp:I-A$^b$-specific naive cells varied markedly in size, ranging from 30–3,000 cells, and composition (Figure 3C). One population consisted of 96% Th1 cells and another of 59% GC-Tfh cells (Figure 3D). In contrast, the effector cell populations derived from the 50 naive cells of recipient origin were very consistent in composition. Th1 cells were the prevalent effector cell type in 15 mice (Figures 2A and 3D). The mean percentages (±SD) for the 20 single donor cell-derived populations were 52% ± 32% Th1, 21% ± 15% Tfh, and 27% ± 26% GC-Tfh cells, whereas those of recipient origin were 57% ± 9% Th1, 20% ± 4% Tfh, and 22% ± 7% GC-Tfh cells. Thus, the mean percentages of Th1, Tfh, and GC-Tfh cells derived from single donor naive cells were very similar to those derived from the 50 naive cells of the recipient, but the variances were significantly greater (F-test of equality of variances, $p < 0.0001$). Taking into account proliferation, the total number of clonally derived Th1, Tfh, and GC-Tfh cells in different mice varied by up to 1,000-fold, whereas the polyclonally derived cells only varied 10-fold (Figure 3E). Thus, individual naive cell clones within a polyclonal repertoire generated different burst sizes and effector cell populations, which averaged together to produce a consistent pattern between individuals.

## Different Single Naive T Cells with the Same TCR Produce Similar Types of Effector Cells

The clonal variation in effector cell generation could have been due to an intrinsic property of the unique TCR expressed by each naive cell or to an extrinsic factor from the environment, such as cytokines. The TCR intrinsic model predicts that single cells with the same TCR should produce similar effector cell types in different instances. We tested this possibility by tracking the fates of single T cells from monoclonal TCR transgenic (Tg) mice after transfer into B6 mice. Initial experiments involved the LCMV GP66:I-A$^b$-specific SMARTA strain (Oxenius et al., 1998) because single monoclonal cells could be compared to single polyclonal T cells of the same specificity.

The GP66:I-A$^b$-specific naive cells of recipient origin consistently produced effector cell populations of about 200,000 cells, composed of 48% ± 3% (mean ± SD) Th1, 37% ± 4% Tfh, and 14% ± 2% GC-Tfh cells on day 8 after LCMV infection (Figures 4A and 4B). There were more Th1 than Tfh than GC-Tfh in every mouse (Figure 4B). In contrast, GP66:I-A$^b$-specific T cell populations generated from eight different single donor naive cells from B6 mice varied markedly in size, ranging from 10–3,000 cells (Figure 4A). Furthermore, the effector cell patterns generated by the single GP66:I-A$^b$-specific naive B6 cells varied greatly, with some clones producing more Tfh than Th1 cells. The means for the eight populations—43% ± 19% (mean ± SD) Th1, 35% ± 13% Tfh, and 20% ± 11% GC-Tfh cells—were very similar to those for the recipient cell-derived populations, whereas the variances were significantly greater (F-test, $p < 0.002$). Thus, single GP66:I-A$^b$-specific T cells from the polyclonal repertoire showed the same variable behavior during LCMV infection that LLOp:I-A$^b$-specific T cells exhibited during Lm infection.

Single SMARTA cells generated more consistent effector cell patterns than single B6 cells. Although eight single SMARTA cells produced 30–3,000 effector cells on day 8 in different LCMV-infected recipients, 6 of 8 cells produced a Th1 > Tfh > GC-Tfh pattern (Figures 4A and 4B). The tendency to produce certain types of effector cells was even more evident for ovalbumin peptide:I-A$^b$-specific OT-II (Barnden et al., 1998), I-Eα chain peptide (Eα):I-A$^b$-specific TEa (Grubin et al., 1997), and FliCp:I-A$^b$-specific SM1 (McSorley et al., 2002) TCR Tg T cells. Most single cells from all three TCR Tg strains expanded about 40-fold after infection with Lm bacteria that expressed the appropriate peptides although some cells, in particular SM1 cells, expanded much more (Figure 4C). Fifteen of 16 single naive OT-II cells generated effector cell populations with a Th1 < Tfh > GC-Tfh pattern. Fourteen of 15 single naive TEa cells produced effector cell populations with a Th1 > Tfh > GC-Tfh pattern, whereas 12 single naive SM1 cells produced either a Th1 < Tfh < GC-Tfh or Th1 < Tfh > GC-Tfh pattern. Thus, single naive T cells from TCR Tg strains produced only 1 or 2 effector cell patterns (Figures 4B and 4D), whereas single naive T cells from the polyclonal LLOp:I-A$^b$-specific repertoire produced many patterns (Figures 3C and 3E). These results were consistent with possibility that the unique TCR expressed by a naive T cell influences its effector cell differentiation pattern.

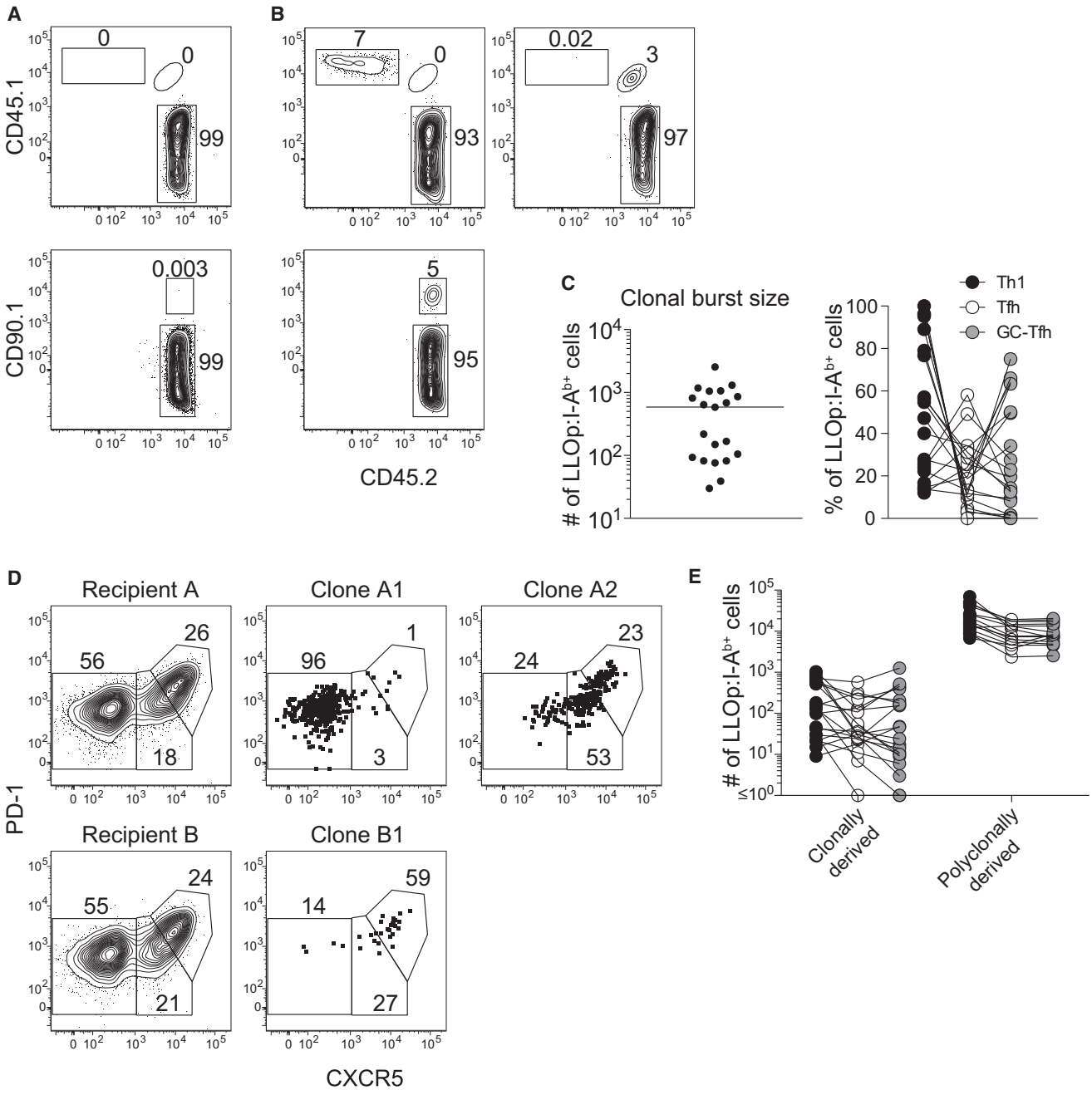


**Figure 3. Single Naive CD4$^+$ T Cells from the Polyclonal Repertoire Exhibit Unique Patterns of Effector Cell Differentiation after Lm Infection**

(A) Plots showing the CD45.1, CD45.2, and CD90.1 staining for LLOp:I-A$^b$-specific cells from B6 mice that did not receive a T cell transfer.

(B) Plots showing CD45.1, CD45.2, and CD90.1 staining for LLOp:I-A$^b$-specific cells from day 7 Lm-infected B6 mice that received a mixture of limiting numbers of CD4$^+$ T cells from CD45.1$^{+/+}$, CD45.1$^+$/CD45.2$^+$, and CD90.1$^{+/+}$ donor mice before infection. CD45.1$^{+/+}$, CD45.1$^+$/CD45.2$^+$, or CD90.1$^{+/+}$ donor-derived cells are shown in the top left, top right, and bottom panels, respectively.

(C) The number (left) and Th1/Tfh/GC-Tfh composition (right) of LLOp:I-A$^b$-specific cells derived from 20 different donor clones identified as in (B).

(D) Plots of CXCR5 and PD-1 staining for donor- or recipient-derived populations from mice described in (B). Recipient A had two different donor cell-derived populations (A1 and A2), whereas Recipient B had only one (B1).

(E) Absolute numbers of clonally derived (donor) or polyclonally derived (recipient) Th1 (black circles), Tfh (white circles), and GC-Tfh (gray circles) LLOp:I-A$^b$-specific cells from day 7 Lm-infected B6 mice that received a mixture of limiting numbers of donor CD4$^+$ T cells before infection. Lines connect values for the same population of LLOp:I-A$^b$-specific cells.

**Table 1. *Tcrb-VDJ* Sequences from Single Cells Demonstrate Clonality of Donor Populations**

| | Frequency | *Tcrb-V* | *Tcrb-D* | *Tcrb-J* | CDR3β |
|---|---|---|---|---|---|
| Random $CD4^+$ | 1 of 10 | 3 | 1 | 1-1 | CASSLDTEVFF |
| | 1 of 10 | 5 | 2 | 2-3 | CASRGLGEAETLYF |
| | 1 of 10 | 5 | 2 | 2-5 | CASSQEDWGGRDTQYF |
| | 1 of 10 | 13-1 | 2 | 2-5 | CASSGDWGAQDTQYF |
| | 1 of 10 | 13-1 | 2 | 2-7 | CASSDVGGYEQYF |
| | 1 of 10 | 13-2 | 2 | 2-5 | CASGGLGGRTQYF |
| | 1 of 10 | 13-2 | 1 | 1-2 | CASGDQGQGAGSDYTF |
| | 1 of 10 | 15 | 1 | 2-5 | CASRGHLQDTQYF |
| | 1 of 10 | 15 | 1 | 1-1 | CASSLQGANTEVFF |
| | 1 of 10 | 16 | 1 | 1-3 | CASSSRISGNTLYF |
| Polyclonal LLOp:I-$A^b$- Specific | 9 of 22 | 14 | 1 | 1-6 | CASSRQGSYEQYF |
| | 4 of 22 | 4 | 2 | 2-7 | CASSRDWGGYEQYF |
| | 3 of 22 | 14 | 1 | 1-1 | CASSFQGAEVFF |
| | 2 of 22 | 15 | 1 | 1-1 | CASRPGQGGRSLF |
| | 1 of 22 | 19 | 2 | 2-7 | CASSIALGTGYEQYF |
| | 1 of 22 | 5 | 1 | 2-5 | CASSPQGDTQYF |
| | 1 of 22 | 5 | 2 | 2-7 | CASSHSDWGAYEQYF |
| | 1 of 22 | 1 | 1 | 2-2 | CTCSAGQANTGQLYF |
| Donor Population 1 | 13 of 13 | 19 | 2 | 2-5 | CASSPQGSGNTLYF |
| Donor Population 2 | 7 of 7 | 14 | 2 | 2-7 | CASSSIYEQYF |
| Donor Population 3 | 18 of 18 | 13-3 | 2 | 2-4 | CASTALGNQNTLYF |
| Donor Population 4 | 7 of 7 | 13-1 | 1 | 1-6 | CASSDLQYNSPLYF |

The sequences shown are from single randomly selected $CD4^+$ T cells (random $CD4^+$), single LLOp:I-$A^b$-tetramer binding $CD4^+$ T cells from day 7 Lm-infected mice (polyclonal LLOp:I-$A^b$-specific), or from single cells of donor origin in day 7 Lm-infected mice that received limiting numbers of donor cells (donor populations 1–4).

## Antigen Dose Influences the Pattern of Effector Cell Differentiation

Different TCRs could influence effector cell differentiation by transducing signals of different strengths. If so, then T cells with a fixed TCR would be expected to produce different types of effector cells when stimulated by different amounts of p:MHCII ligand. This scenario was tested by infecting B6 mice containing about 100 SM1 TCR Tg cells with $10^7$ Lm-FliC, $10^6$ Lm-FliC plus $9 \times 10^6$ Lm, or $10^5$ Lm-FliC plus $9.9 \times 10^6$ Lm bacteria. This setup produced a situation in which FliCp:I-$A^b$ complexes were varied, but the total amount of Lm bacteria and the associated inflammation were kept constant. Twenty-five thousand Th1 cells were generated 7 days after infection with $10^5$ Lm-FliC bacteria (Figure 5A). The number of Th1 cells rose to 83,000 after infection with $10^6$ and then fell to 23,000 after infection with $10^7$ Lm-FliC bacteria. In contrast, the number of Tfh cells went from 16,000 after infection with $10^5$ Lm-FliC bacteria to 58,000 after infection with $10^6$ and 52,000 with $10^7$. Similarly, the number of GC-Tfh cells went from 2,000 at the $10^5$ dose to 16,000 and 39,000 at the $10^6$ and $10^7$ doses, respectively. A similar pattern was observed in the liver, a site of Lm replication (Portnoy et al., 2002), except that very few Tfh and even fewer GC-Tfh migrated to this organ. Thus, the reduction in Th1 cells in the lymphoid organs after infection with $10^7$ Lm-FliC bacteria was not due to selective migration to nonlymphoid tissues. The $CXCR5^-$ cells expressed more T-bet than the $CXCR5^+$ cells in every case, indicating that the $CXCR5^-$ cells were Th1 cells even at the highest Lm-FliC dose, where their numbers declined (Figure 5B). These results demonstrated that Th1 cell formation increased with antigen dose until a point and then decreased, whereas Tfh and GC-Tfh generation increased progressively. This pattern is consistent with a model in which strong TCR signaling inhibits Th1 formation and favors Tfh and GC-Tfh formation.

The effect of antigen dose on T-bet and Bcl-6 expression was measured to test this model. T-bet was induced in SM1 cells in the secondary lymphoid organs, 2.5 days after infection with $10^5$ Lm-FliC bacteria, increased after infection with $10^6$ bacteria, and declined after infection with $10^7$ bacteria (Figure 5C). In contrast, Bcl-6 expression increased progressively as the number of bacteria was increased. These results support the model in which effector cells are diverted from the Th1 to the Tfh and GC-Tfh fates in response to high TCR signaling.

## TCR-p:MHCII Dwell Time Influences the Pattern of Effector Cell Differentiation

The antigen dose results implied that TCR signal strength influences the effector cell differentiation pattern. If so, then naive cells in a polyclonal repertoire might receive different signal strengths and adopt different effector cell patterns based on the binding properties of their TCRs to p:MHCII. Two TCR-p:MHC binding parameters have been suggested to influence

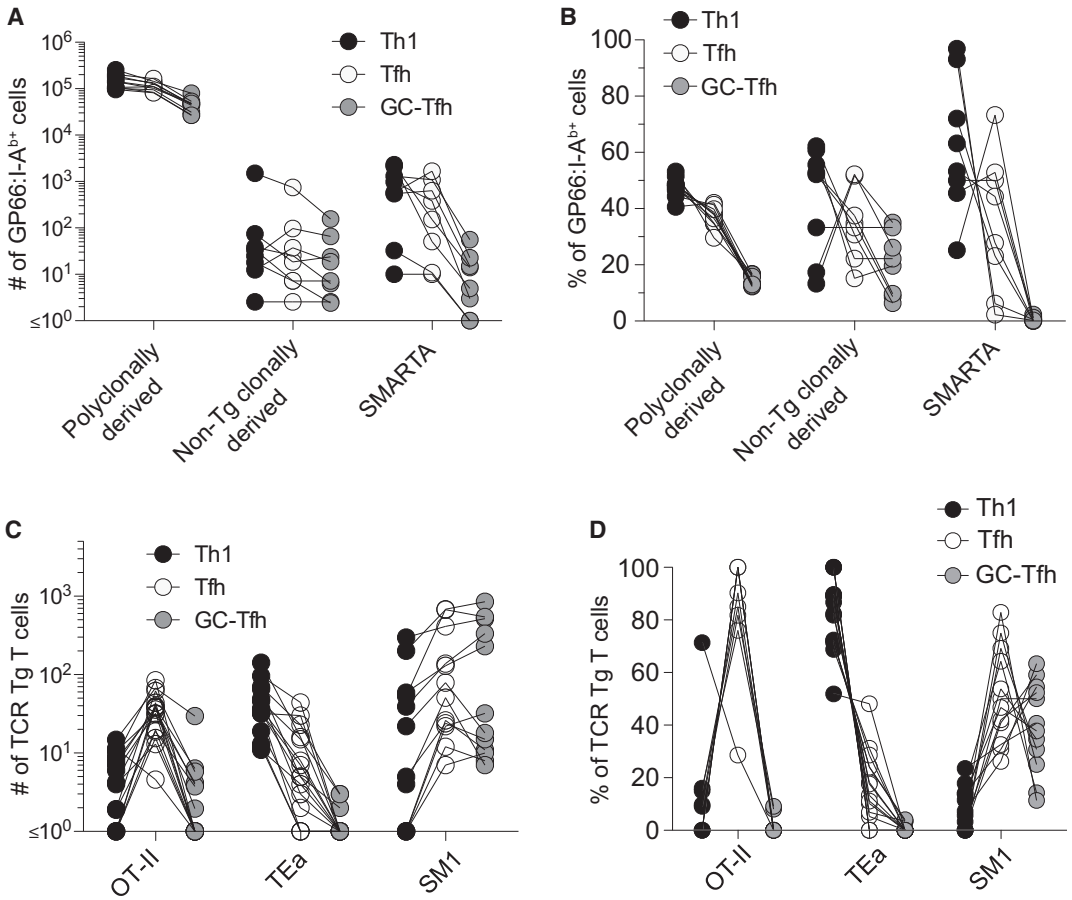


**Figure 4. Single Naive Monoclonal CD4$^+$ T Cells from TCR Tg Mice Exhibit Similar Patterns of Effector Cell Differentiation**

(A and B) Numbers (A) and percentages (B) of Th1 (black circles), Tfh (white circles), and GC-Tfh (gray circles) from GP66:I-A$^b$-specific cell populations derived from the intact polyclonal repertoires of recipient mice, single donor cells from B6 mice, or single donor cells from SMARTA mice, 8 days after LCMV infection. (C and D) Numbers (C) and percentages (D) of Th1 (black circles), Tfh (white circles), or GC-Tfh (gray circles) cells derived from single naive OT-II, TEa, or SM1 cells, 7 days after infection with $10^7$ Lm-2W, Lm-E$\alpha$, or Lm-FliC bacteria, respectively. Each connecting line in (A, B, C, and D) represents a single population.

T cell responses. The receptor occupancy model suggests that ligand potency is a function of TCR-p:MHC equilibrium affinity ($K_D$). In contrast, the kinetic proofreading model posits that ligand potency depends on the half-life ($t_{1/2}$) of the TCR-p:MHC interaction because the TCR must bind to p:MHC long enough to complete a series of signaling events. Neither model, however, perfectly predicts ligand potency (Kersh et al., 1998; Krogsgaard et al., 2003). Recently, a variation of the kinetic proofreading model has been proposed to account for this discrepancy. This model suggests that TCRs that have fast on-rates can bind and rebind rapidly to the same p:MHCII ligand several times in the immunological synapse before diffusing away (Aleksic et al., 2010; Govern et al., 2010). Rebinding leads to an aggregate $t_{1/2}$ ($t_a$) that can be longer than the conventional $t_{1/2}$ for TCRs with fast on-rates. The $t_a$ has been shown to be a better predictor of T cell proliferation than $K_D$ or $t_{1/2}$ (Govern et al., 2010; Vanguri et al., 2013).

We assessed these models using two TCR Tg lines called B3K506 and B3K508 (Huseby et al., 2005). The B3K506 and B3K508 TCRs bind to a set of I-A$^b$-bound peptides called 3K, P5R, and P-1A with known $t_a$ and $K_D$ values (Govern et al., 2010). Importantly, these peptides bind I-A$^b$ equivalently (Govern et al., 2010). The receptor occupancy model was tested by determining whether the intensity of p:MHCII tetramer staining, which is related to $K_D$ (Crawford et al., 1998), correlated with effector cell differentiation pattern. B3K506 T cells bound about four times more 3K:I-A$^b$ tetramer than B3K508 T cells, which corresponded with the B3K506 TCR having a 4-fold higher affinity for 3K:I-A$^b$ than the B3K508 TCR (Govern et al., 2010), while neither T cell population bound to FliCp:I-A$^b$ tetramer (Figure 6A). However, B3K508 or B3K506 T cells generated a similar effector cell pattern in adoptive recipients infected with Lm-3K bacteria (Figure 6B). Thus, a pure affinity-based TCR occupancy model did not fit the effector cell differentiation results.

The kinetic proofreading model based on TCR dwell time on p:MHCII was then tested by determining whether $t_a$ correlated with effector cell differentiation patterns. Indeed, this was the case as evidenced by the finding that the B3K508 and B3K506 TCRs, which generated a similar effector cell pattern in response to Lm-3K infection, have similar $t_a$s of 2.8 and 3.1 s (Govern et al.,

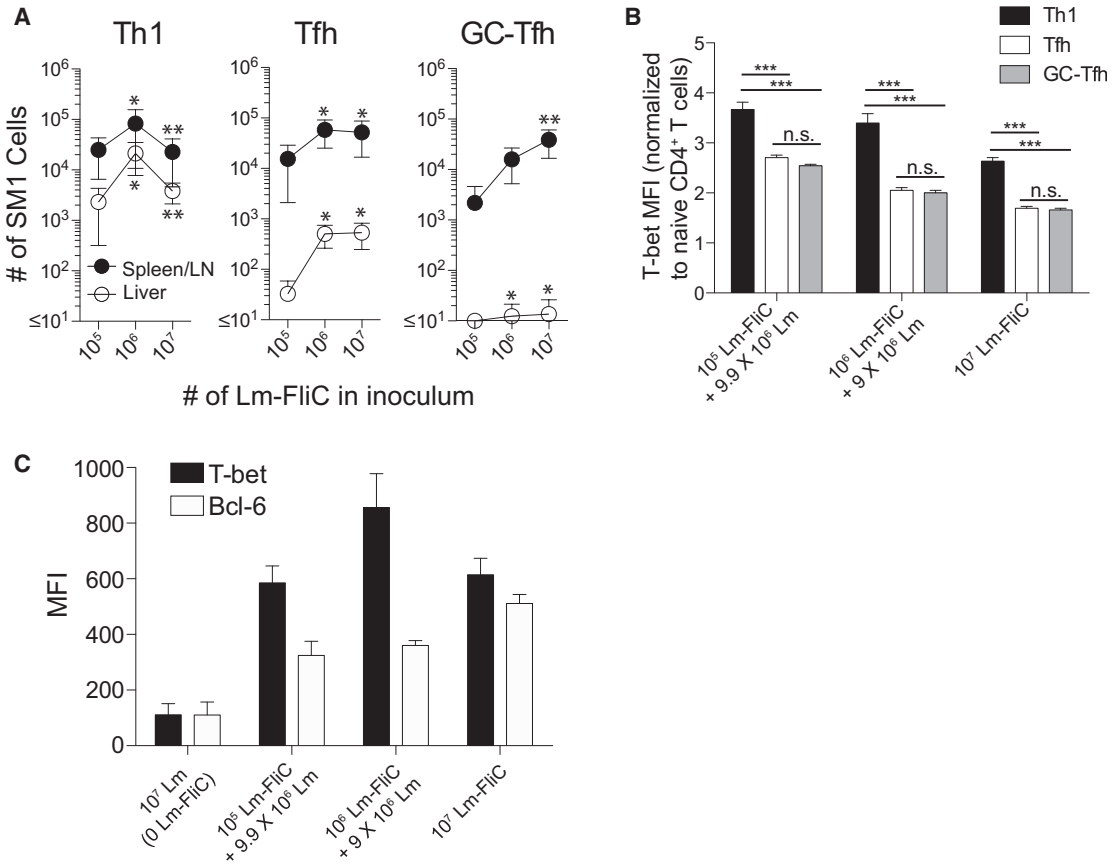


**Figure 5. Antigen Dose Influences the Differentiation of Monoclonal CD4⁺ T Cells**

(A) Number ± SD ($n \geq 8$) of Th1 (left), Tfh (middle), and GC-Tfh (right) SM1 TCR Tg cells in the spleen and LN (black dots) and livers (white dots) of B6 mice initially containing 100 naive SM1 cells 7 days after infection with the indicated bacteria. The asterisk denotes significant difference ($p < 0.05$) compared to $10^5$ Lm-FliC dose, and the double asterisk denotes significant difference ($p < 0.05$) compared to $10^6$ Lm-FliC dose.

(B) T-bet mean fluorescence intensity (MFI) (normalized to T-bet MFI in naive CD4⁺ T cells) ± SD ($n = 3$) of SM1 cells that were Th1 (black bars), Tfh (white bars), or GC-Tfh (gray bars) cells in spleen and LN of individual animals infected 7 days earlier with the indicated bacteria. Results are representative of three independent experiments. ***$p < 0.001$.

(C) T-bet and Bcl-6 MFI of SM1 cells in the spleens of B6 mice ($n = 4$–5) that initially contained 100 naive SM1 cells, 60 hr after infection. All statistics performed using one-way ANOVA, Bonferroni's multiple comparison test.

2010) (Figure 6B). In contrast, the B3K508 and B3K506 TCRs, which bind P5R:I-$A^b$ with different $t_a$s of 0.9 and 2.3 s (Govern et al., 2010), generated different effector cell patterns in response to Lm-P5R infection (Figure 6C). The correspondence between $t_a$ and effector cell differentiation held for all five of the TCR-p:MHCII combinations tested (Figure 6D) and in the complex fashion noted in the antigen dose response experiments (Figure 5A). The number of Th1 cells increased from a low level for TCR-p:MHCII dwell times of 0.9 s to a much higher level for a dwell time of 2.3 s and then decreased for dwell times of about 3 s. In contrast, Tfh and GC-Tfh formation increased between dwell times of 0.9 and 2.3 s and then plateaued. Although the Th1 pattern fit poorly to a linear function (data not shown), all patterns fit extremely well with second-order polynomial functions ($r^2$ = 0.87–0.99). The remarkable similarity between the effects of increasing antigen dose (Figure 5A) or $t_a$ (Figure 6D) suggests that CD4⁺ T cell differentiation is influenced by p:MHCII density and TCR-p:MHCII dwell time.

## DISCUSSION

Our studies confirmed earlier observations on CD8⁺ T cells (Gerlach et al., 2010; Stemberger et al., 2007) by showing that single naive CD4⁺ T cells could produce different types of effector cells. However, our studies provide the additional insight that the TCR on each naive CD4⁺ T cell can instruct this behavior based on dwell time on p:MHCII or p:MHCII density. This conclusion is based on the finding that the $t_a$ of a TCR-p:MHCII interaction and the antigen dose predicted the effector cell pattern. The $t_a$ takes into account TCR binding and rebinding to p:MHCII in the two-dimensional space of the opposed T cell and APC membranes in which diffusion is limited (Aleksic et al., 2010; Govern et al., 2010). Rebinding is predicted to occur so rapidly that it would be perceived by the TCR signaling apparatus as continuous binding. Thus, effectively long dwell times on p:MHCII can be achieved by TCRs with long $t_a$s due to fast on-rates and rebinding (B3K506-3K:I-$A^b$) or by TCRs with slow on-rates

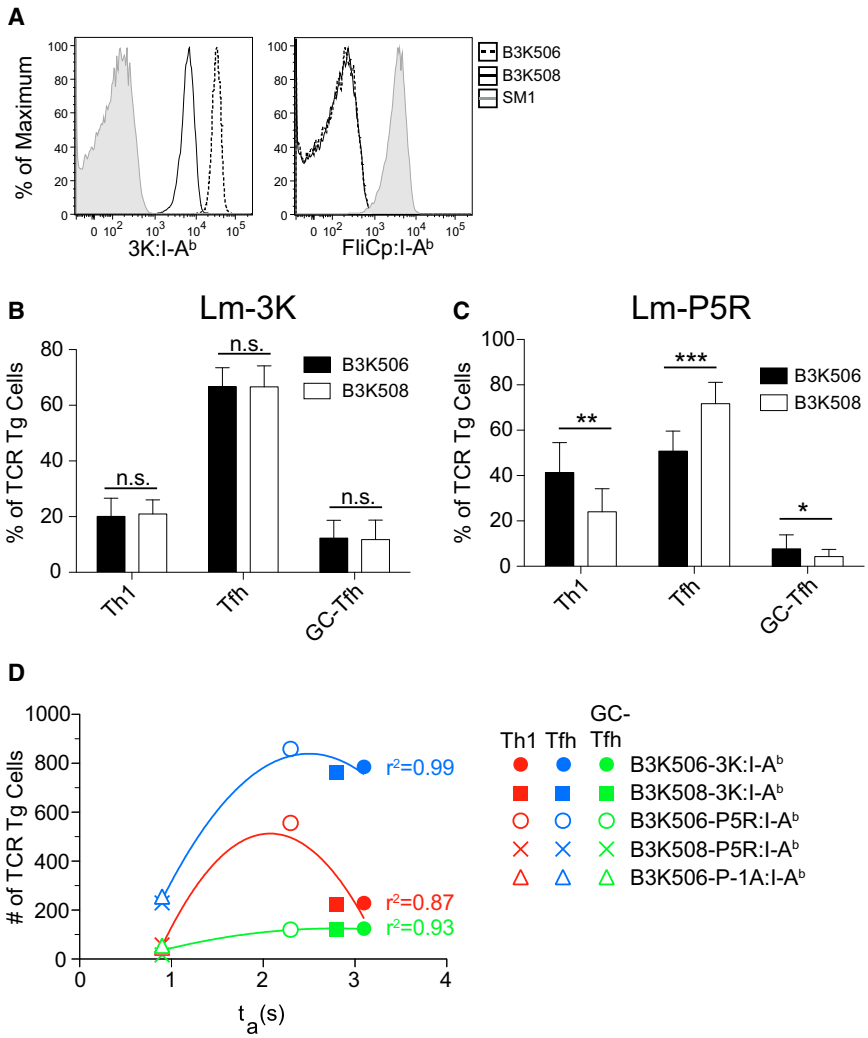


**Figure 6. Effector Differentiation Correlates with TCR-p:MHCII Dwell Time**

(A) 3K:I-$A^b$ (left) or FliCp:I-$A^b$ (right) tetramer staining of B3K506 (dashed line), B3K508 (solid line), or SM1 (shaded) T cells.

(B and C) Percentage ± SD ($n \geq 8$) of B3K506 (black bars) or B3K508 (white bars) T cells that were Th1, Tfh, or GC-Tfh cells in adoptive B6 hosts, 7 days after Lm-3K (B) or Lm-P5R (C) infection. p values from paired t tests, *$p < 0.05$, **$p < 0.01$, and ***$p < 0.001$.

(D) Number of Th1 (red), Tfh (blue), or GC-Tfh (green) cells normalized to the number of transferred naive cells and derived from the indicated TCR-p:MHCII interactions, plotted versus $t_a$ values (Govern et al., 2010). The data were fit to second-order polynomial functions. $r^2$ values are shown for each curve. Each symbol is defined on the plot and represents the average values from 6–10 mice.

and slow off-rates (B3K508-3K:I-$A^b$), for which rebinding is not predicted to occur. The fact that $t_a$ is a better indicator of TCR signaling than equilibrium affinity ($K_D$) (Govern et al., 2010; Vanguri et al., 2013) may explain why p:MHCII tetramer binding, which relates to $K_D$ (Crawford et al., 1998), correlates with T cell activation in some cases (Fazilleau et al., 2009), but not others (Derby et al., 2001; Kersh et al., 1998; Speiser et al., 2008).

The relationship between TCR-p:MHCII dwell time and effector cell differentiation was complex. Two different TCR-p:MHCII interactions with short dwell times supported weak clonal expansion of all effector cell types, an interaction with an intermediate dwell time produced maximal expansion and the most Th1 cells, whereas two different interactions with long dwell times suppressed Th1 cells, thereby favoring Tfh and GC-Tfh cells. T cells with long dwell time TCRs may be directed to the GC-Tfh fate to maximize affinity maturation by providing help to germinal center B cells as antigen becomes limiting.

None of the five B3K506 or B3K508 TCR-p:MHCII interactions produced the predominant Th1 cell pattern observed for certain naive cells from the polyclonal repertoire. This pattern may be induced by TCR-p:MHCII dwell times that lie in the 0.9–2.3 s interval that could not be tested with the B3K506/B3K508 system.

TCR-p:MHCII dwell time may influence effector cell differentiation by regulation of the IL-2 receptor (Choi et al., 2011; Pepper et al., 2011; Yu et al., 2009). TCR signaling induces IL-2 receptor, T-bet, and Bcl-6 expression by all naive T cells (Nakayamada et al., 2011; Oestreich et al., 2012). As early as the second division, however, cells either maintain expression of the IL-2 receptor or lose it (Choi et al., 2011; Pepper et al., 2011) in a way that may be controlled by TCR signal strength. Strong TCR signaling can cause asymmetric cell division that promotes unequal partitioning of the IL-2 receptor into daughter cells (Chang et al., 2007; King et al., 2012). The daughter cells that inherit the IL-2 receptor would then receive STAT5 signals and induce the IL-12 receptor and Blimp1. These events would lead to the suppression of Bcl-6, induction of T-bet, and Th1 cell formation (Johnston et al., 2009) (Nakayamada et al., 2011). The daughter cells that do not inherit the IL-2 receptor would not receive STAT5 signals or suppress Bcl-6 and become Tfh or GC-Tfh cells. Alternatively, strong TCR signals have been shown to uncouple the IL-2 receptor from the STAT5 signaling pathway (Yamane et al., 2005), thereby interrupting the positive feedback that maintains IL-2 receptor, thereby promoting the Tfh and GC-Tfh fates.

In either case, the T cells in a polyclonal repertoire that have TCRs capable of long dwell times on p:MHCII are predicted to receive the strongest signals and become GC-Tfh effector cells as proposed by others (Deenick et al., 2010; Fazilleau et al., 2009). This concept can explain why different LLOp:I-$A^b$-specific naive T cells from the polyclonal repertoire produced different effector patterns in the same infection. Similarly, GC-Tfh effector

cell formation would become more likely at high antigen dose as all T cells in the population are confronted with APC displaying larger numbers of p:MHCII. It is thus possible that the LLOp:I-$A^b$ and 2W:I-$A^b$ epitopes consistently induced different effector T cell patterns because of different amounts of presentation during infection.

It is important to note that intrinsic TCR-p:MHCII dwell time was not the only driver of effector cell differentiation. This point was evident in the variability in effector cell generation from different single naive T cells with the same TCR. For example, although most OT-II cells produced very few Th1 cells after Lm infection, one clone produced 70% Th1 cells, and SMARTA cells produced several effector cell patterns. In addition, some single TCR Tg T cells produced ten progeny, whereas others produced 3,000. This variability could be due to individual naive T cells encountering APC that vary with respect to cytokine production, costimulatory molecules, and/or p:MHCII display. Differences in these extrinsic factors would be expected to influence effector cell differentiation no matter which TCR the T cell expresses.

TCR-based control of effector cell patterning provides an explanation for the curious variability of the FliCp:I-$A^b$-specific T cell response. Consider a case in which each mouse has only two naive p:I-$A^b$-specific T cells. Because of the random process of *Tcr* gene segment assembly the two cells would likely have different TCRs with different intrinsic p:MHCII dwell times. If by chance, the two TCRs had long dwell times, then Tfh and GC-Tfh cell production would be favored, whereas Th1 cell formation would prevail if the two TCRs had intermediate dwell times. This variability would not occur for a large naive cell population as it becomes impossible for all of its TCRs to by chance have the same dwell time. This phenomenon may explain why elite control of HIV infection correlates with certain TCR clonotypes (Chen et al., 2012). The number of relevant naive T cells may be so small that chance differences in TCR composition and associated signaling potential might produce highly cytotoxic effector cells in some people, but not others. A similar phenomenon may explain how identical twins can be discordant for autoimmune disease (Utz et al., 1993).

## EXPERIMENTAL PROCEDURES

### Mice

Six- to 8-week-old C57BL/6 (B6), B6.SJL-*Ptprc*$^a$ *Pep3*$^b$/BoyJ (CD45.1), and B6.PL-*Thy1a*/CyJ (CD90.1) mice were purchased from the Jackson Laboratory (Bar Harbor, ME, USA) or the National Cancer Institute Mouse Repository (Frederick, MD, USA). (B6 x B6.SJL-*Ptprc*$^a$ *Pep3*$^b$/BoyJ) (CD45.1 x B6) $F_1$, *Rag1*$^{-/-}$ OT-II (Barnden et al., 1998), *Rag1*$^{-/-}$ SM1 (McSorley et al., 2002), SMARTA (Oxenius et al., 1998), and *Rag1*$^{-/-}$ TEa (Grubin et al., 1997) mice were bred and housed in specific pathogen-free conditions in accordance with guidelines of the University of Minnesota Institutional Animal Care and Use Committee and National Institutes of Health. *Rag1*$^{-/-}$ B3K506 and *Rag1*$^{-/-}$ B3K508 TCR transgenic mice (Huseby et al., 2005) were maintained at the University of Massachusetts Medical School. Spleen cells were shipped overnight to the University of Minnesota and injected into B6 mice as described below.

### Infections

The ActA-deficient Lm, Lm-2W, and Lm-FliC strains were described previously (Ertelt et al., 2009; Johanns et al., 2010). The ActA-deficient Lm-Eα, Lm-3K, Lm-P5R, and Lm-P-1A strains were produced using a similar approach (Ertelt et al., 2009) by ligating the coding sequence for a chicken ovalbumin fragment fused to the I-E alpha chain peptide 52-68 (ASFEAQGALANIAVDKA) (Rudensky et al., 1991), GP66 (DIYKGVYQFKSV), 3K (ASFEAQKAKANKAVDKA), P5R (ASFEAQKARANKAVDKA), or P-1A (ASFAAQKAKANKAVDKA) peptides into the Pst1 and Stu1 restriction sites of the pAM401-based Lm-expression construct. Mice were injected intravenously with Lm bacteria or intraperitoneally with $2 \times 10^5$ plaque-forming units of the LCMV Armstrong strain.

### Tetramers

Biotin-labeled soluble I-$A^b$ molecules containing 2W, LCMV glycoprotein $(GP)_{66-77}$, $LLO_{190-201}$, or $FliC_{427-441}$ peptides covalently attached to the I-$A^b$ beta chain were produced with the I-$A^b$ alpha chain in *Drosophila melanogaster* S2 cells, then purified, and made into tetramers with streptavidin (SA)-phycoerythrin (PE) or (SA)-allophycocyanin (Prozyme, San Leandro, CA, USA) as described previously (Moon et al., 2007; Pepper et al., 2011).

### Cell Enrichment and Flow Cytometry

Single cell suspensions of spleen and LN cells or liver cells were stained for 1 hr at room temperature with allophycocyanin-conjugated tetramers and 2 μg of CXCR5-PE antibody (2G8; Becton Dickinson, Franklin Lakes, NJ, USA). In double tetramer staining experiments, CXCR5-PE antibody was omitted and a second PE-conjugated tetramer was used. Samples were then enriched for bead-bound cells and enumerated as described previously (Moon et al., 2007). For identification of surface markers, the sample was stained on ice with antibodies specific for B220 (RA3-6B2), CD11b (MI-70), CD11c (N418), CD8α (5H10; Invitrogen, Carlsbad, CA, USA), PD-1 (J43), CD4 (RM4-5), CD3ε (145-2C11), CD44 (IM7), CD45.1 (A20), CD45.2 (104), CD90.1 (HIS51), and/or CD90.2 (53-2.1), each conjugated to a different fluorochrome. Intracellular staining for T-bet and Bcl-6 was performed as described previously (Pepper et al., 2011). All antibodies were from eBioscience (San Diego) unless noted. Cells were then analyzed on an LSR II or Fortessa (Becton Dickinson) flow cytometer. Data were analyzed with FlowJo (TreeStar, Ashland, OR, USA).

### Isolation of Liver Resident Lymphocytes

Livers were harvested from perfused animals. Single cell suspensions were prepared by mechanical dissociation of liver tissue through a 70 μM nylon mesh. Liver cells were suspended in 44% Percoll (GE Healthcare, Waukesha, WI, USA) and layered on 67% Percoll. Cells were centrifuged at room temperature for 20 min at 900 times g. Lymphocytes were harvested from the gradient interphase.

### Cell Transfer

Spleens and LN were collected from donor mice, and $CD4^+$ T cells were enriched with a $CD4^+$ T Cell Isolation Kit II (Miltenyi Biotec, Bergisch Gladbach, Germany). For limiting dilution experiments, $CD4^+$ T cells were injected intravenously into recipient mice based on a 10% park rate and the frequency of naive cells specific for the p:MHCII of interest: $7 \times 10^5$ for LLOp:I-$A^b$-specific cells and $6 \times 10^5$ for GP66:I-$A^b$-specific cells.

Single $CD4^+$ TCR Tg T cells were isolated either by cell sorting or limiting dilution. For limiting dilution experiments, two $CD4^+$ TCR Tg cells were injected into each recipient with the assumption that at most 20% of the transferred cells would survive. The percentage of recipient mice containing donor cell-derived progeny was less than 35% in all but one experiment, where it was 68%. For cell-sorting experiments, enriched $CD4^+$ T cells were stained with antibodies specific for CD11b, CD11c, B220, and annexin V (BD) and single $CD11b^-$ $CD11c^-$ $B220^-$ annexin $V^-$ cells were sorted on a BD Aria and injected intravenously into recipient mice.

### *Tcrb* Sequencing

The method of Dash and colleagues (Dash et al., 2011) was used to obtain *Tcrb-VDJ* sequences from single cells. PCR products were sequenced with an Applied Biosystems (Foster City, CA, USA) Prism 3730xl at the University of Minnesota BioMedical Genomics Center. Sequences were analyzed using Applied Biosystems Sequence Scanner software, and a section of unambiguous sequence (typically base pairs 25–275) was analyzed using the

Immunogenetics Information system (http://www.IMGT.org) V-quest alignment software.

### Statistical Analysis

Statistical tests were performed using Prism (Graphpad) software.

## ACKNOWLEDGMENTS

We thank J. Walter and R. Speier for technical assistance and T. Martin and the University of Minnesota Flow Cytometry Facility for cell sorting. This work was supported by grants from the National Institutes of Health (R01-AI39614, R37-AI27998, and R01-AI66018 to M.K.J.; T32-HD060536 to N.J.T.; T32-AI07313 to A.J.P.; F30-DK093242 to R.W.N.; R01-AI087830 and R01-AI100934 to S.S.W.; and T32-AI07313 to J.L.L.). This work was also supported by the Kunze Fellowship (to A.J.P.), the Irvington Fellowship from the Cancer Research Institute (to J.J.T.), and the Burroughs Wellcome Fund (to S.S.W.).

Received: August 4, 2012
Revised: November 5, 2012
Accepted: April 4, 2013
Published: May 9, 2013

## REFERENCES

Aleksic, M., Dushek, O., Zhang, H., Shenderov, E., Chen, J.L., Cerundolo, V., Coombs, D., and van der Merwe, P.A. (2010). Dependence of T cell antigen recognition on T cell receptor-peptide MHC confinement time. Immunity *32*, 163–174.

Ansel, K.M., McHeyzer-Williams, L.J., Ngo, V.N., McHeyzer-Williams, M.G., and Cyster, J.G. (1999). In vivo-activated CD4 T cells upregulate CXC chemokine receptor 5 and reprogram their response to lymphoid chemokines. J. Exp. Med. *190*, 1123–1134.

Barnden, M.J., Allison, J., Heath, W.R., and Carbone, F.R. (1998). Defective TCR expression in transgenic mice constructed using cDNA-based alpha- and beta-chain genes under the control of heterologous regulatory elements. Immunol. Cell Biol. *76*, 34–40.

Bretscher, P.A., Wei, G., Menon, J.N., and Bielefeldt-Ohmann, H. (1992). Establishment of stable, cell-mediated immunity that makes "susceptible" mice resistant to Leishmania major. Science *257*, 539–542.

Chang, J.T., Palanivel, V.R., Kinjyo, I., Schambach, F., Intlekofer, A.M., Banerjee, A., Longworth, S.A., Vinup, K.E., Mrass, P., Oliaro, J., et al. (2007). Asymmetric T lymphocyte division in the initiation of adaptive immune responses. Science *315*, 1687–1691.

Chen, H., Ndhlovu, Z.M., Liu, D., Porter, L.C., Fang, J.W., Darko, S., Brockman, M.A., Miura, T., Brumme, Z.L., Schneidewind, A., et al. (2012). TCR clonotypes modulate the protective effect of HLA class I molecules in HIV-1 infection. Nat. Immunol. *13*, 691–700.

Choi, Y.S., Kageyama, R., Eto, D., Escobar, T.C., Johnston, R.J., Monticelli, L., Lao, C., and Crotty, S. (2011). ICOS receptor instructs T follicular helper cell versus effector cell differentiation via induction of the transcriptional repressor Bcl6. Immunity *34*, 932–946.

Constant, S., Pfeiffer, C., Woodard, A., Pasqualini, T., and Bottomly, K. (1995). Extent of T cell receptor ligation can determine the functional differentiation of naive CD4+ T cells. J. Exp. Med. *182*, 1591–1596.

Crawford, F., Kozono, H., White, J., Marrack, P., and Kappler, J. (1998). Detection of antigen-specific T cells with multivalent soluble class II MHC covalent peptide complexes. Immunity *8*, 675–682.

Crotty, S. (2011). Follicular helper CD4 T cells (TFH). Annu. Rev. Immunol. *29*, 621–663.

Dash, P., McClaren, J.L., Oguin, T.H., 3rd, Rothwell, W., Todd, B., Morris, M.Y., Becksfort, J., Reynolds, C., Brown, S.A., Doherty, P.C., and Thomas, P.G. (2011). Paired analysis of TCRα and TCRβ chains at the single-cell level in mice. J. Clin. Invest. *121*, 288–295.

Davis, M.M., Boniface, J.J., Reich, Z., Lyons, D., Hampl, J., Arden, B., and Chien, Y. (1998). Ligand recognition by alpha beta T cell receptors. Annu. Rev. Immunol. *16*, 523–544.

Deenick, E.K., Chan, A., Ma, C.S., Gatto, D., Schwartzberg, P.L., Brink, R., and Tangye, S.G. (2010). Follicular helper T cell differentiation requires continuous antigen presentation that is independent of unique B cell signaling. Immunity *33*, 241–253.

Derby, M.A., Wang, J., Margulies, D.H., and Berzofsky, J.A. (2001). Two intermediate-avidity cytotoxic T lymphocyte clones with a disparity between functional avidity and MHC tetramer staining. Int. Immunol. *13*, 817–824.

Ertelt, J.M., Rowe, J.H., Johanns, T.M., Lai, J.C., McLachlan, J.B., and Way, S.S. (2009). Selective priming and expansion of antigen-specific Foxp3- CD4+ T cells during Listeria monocytogenes infection. J. Immunol. *182*, 3032–3038.

Fazilleau, N., McHeyzer-Williams, L.J., Rosen, H., and McHeyzer-Williams, M.G. (2009). The function of follicular helper T cells is regulated by the strength of T cell antigen receptor binding. Nat. Immunol. *10*, 375–384.

Geginat, G., Schenk, S., Skoberne, M., Goebel, W., and Hof, H. (2001). A novel approach of direct ex vivo epitope mapping identifies dominant and subdominant CD4 and CD8 T cell epitopes from Listeria monocytogenes. J. Immunol. *166*, 1877–1884.

Gerlach, C., van Heijst, J.W., Swart, E., Sie, D., Armstrong, N., Kerkhoven, R.M., Zehn, D., Bevan, M.J., Schepers, K., and Schumacher, T.N. (2010). One naive T cell, multiple fates in CD8+ T cell differentiation. J. Exp. Med. *207*, 1235–1246.

Govern, C.C., Paczosa, M.K., Chakraborty, A.K., and Huseby, E.S. (2010). Fast on-rates allow short dwell time ligands to activate T cells. Proc. Natl. Acad. Sci. USA *107*, 8724–8729.

Grubin, C.E., Kovats, S., deRoos, P., and Rudensky, A.Y. (1997). Deficient positive selection of CD4 T cells in mice displaying altered repertoires of MHC class II-bound self-peptides. Immunity *7*, 197–208.

Hosken, N.A., Shibuya, K., Heath, A.W., Murphy, K.M., and O'Garra, A. (1995). The effect of antigen dose on CD4+ T helper cell phenotype development in a T cell receptor-alpha beta-transgenic model. J. Exp. Med. *182*, 1579–1584.

Huseby, E.S., White, J., Crawford, F., Vass, T., Becker, D., Pinilla, C., Marrack, P., and Kappler, J.W. (2005). How the T cell repertoire becomes peptide and MHC specific. Cell *122*, 247–260.

Itano, A.A., and Jenkins, M.K. (2003). Antigen presentation to naive CD4 T cells in the lymph node. Nat. Immunol. *4*, 733–739.

Jenkins, M.K., Chu, H.H., McLachlan, J.B., and Moon, J.J. (2010). On the composition of the preimmune repertoire of T cells specific for Peptide-major histocompatibility complex ligands. Annu. Rev. Immunol. *28*, 275–294.

Johanns, T.M., Ertelt, J.M., Lai, J.C., Rowe, J.H., Avant, R.A., and Way, S.S. (2010). Naturally occurring altered peptide ligands control Salmonella-specific CD4+ T cell proliferation, IFN-gamma production, and protective potency. J. Immunol. *184*, 869–876.

Johnston, R.J., Poholek, A.C., DiToro, D., Yusuf, I., Eto, D., Barnett, B., Dent, A.L., Craft, J., and Crotty, S. (2009). Bcl6 and Blimp-1 are reciprocal and antagonistic regulators of T follicular helper cell differentiation. Science *325*, 1006–1010.

Johnston, R.J., Choi, Y.S., Diamond, J.A., Yang, J.A., and Crotty, S. (2012). STAT5 is a potent negative regulator of TFH cell differentiation. J. Exp. Med. *209*, 243–250.

Kersh, G.J., Kersh, E.N., Fremont, D.H., and Allen, P.M. (1998). High- and low-potency ligands with similar affinities for the TCR: the importance of kinetics in TCR signaling. Immunity *9*, 817–826.

King, C.G., Koehli, S., Hausmann, B., Schmaler, M., Zehn, D., and Palmer, E. (2012). T cell affinity regulates asymmetric division, effector cell differentiation, and tissue pathology. Immunity *37*, 709–720.

Krogsgaard, M., Prado, N., Adams, E.J., He, X.L., Chow, D.C., Wilson, D.B., Garcia, K.C., and Davis, M.M. (2003). Evidence that structural rearrangements and/or flexibility during TCR binding can contribute to T cell activation. Mol. Cell *12*, 1367–1378.

Lee, S.K., Rigby, R.J., Zotos, D., Tsai, L.M., Kawamoto, S., Marshall, J.L., Ramiscal, R.R., Chan, T.D., Gatto, D., Brink, R., et al. (2011). B cell priming for extrafollicular antibody responses requires Bcl-6 expression by T cells. J. Exp. Med. *208*, 1377–1388.

Liao, W., Lin, J.X., Wang, L., Li, P., and Leonard, W.J. (2011). Modulation of cytokine receptors by IL-2 broadly regulates differentiation into helper T cell lineages. Nat. Immunol. *12*, 551–559.

Marrack, P., Scott-Browne, J.P., Dai, S., Gapin, L., and Kappler, J.W. (2008). Evolutionarily conserved amino acids that control TCR-MHC interaction. Annu. Rev. Immunol. *26*, 171–203.

Marshall, H.D., Chandele, A., Jung, Y.W., Meng, H., Poholek, A.C., Parish, I.A., Rutishauser, R., Cui, W., Kleinstein, S.H., Craft, J., and Kaech, S.M. (2011). Differential expression of Ly6C and T-bet distinguish effector and memory Th1 CD4(+) cell properties during viral infection. Immunity *35*, 633–646.

McSorley, S.J., Asch, S., Costalonga, M., Reinhardt, R.L., and Jenkins, M.K. (2002). Tracking salmonella-specific CD4 T cells in vivo reveals a local mucosal response to a disseminated infection. Immunity *16*, 365–377.

Moon, J.J., Chu, H.H., Pepper, M., McSorley, S.J., Jameson, S.C., Kedl, R.M., and Jenkins, M.K. (2007). Naive CD4(+) T cell frequency varies for different epitopes and predicts repertoire diversity and response magnitude. Immunity *27*, 203–213.

Moon, J.J., Dash, P., Oguin, T.H., 3rd, McClaren, J.L., Chu, H.H., Thomas, P.G., and Jenkins, M.K. (2011). Quantitative impact of thymic selection on Foxp3+ and Foxp3- subsets of self-peptide/MHC class II-specific CD4+ T cells. Proc. Natl. Acad. Sci. USA *108*, 14602–14607.

Nakayamada, S., Kanno, Y., Takahashi, H., Jankovic, D., Lu, K.T., Johnson, T.A., Sun, H.W., Vahedi, G., Hakim, O., Handon, R., et al. (2011). Early Th1 cell differentiation is marked by a Tfh cell-like transition. Immunity *35*, 919–931.

Nurieva, R.I., Chung, Y., Hwang, D., Yang, X.O., Kang, H.S., Ma, L., Wang, Y.H., Watowich, S.S., Jetten, A.M., Tian, Q., and Dong, C. (2008). Generation of T follicular helper cells is mediated by interleukin-21 but independent of T helper 1, 2, or 17 cell lineages. Immunity *29*, 138–149.

Oestreich, K.J., Mohn, S.E., and Weinmann, A.S. (2012). Molecular mechanisms that control the expression and activity of Bcl-6 in TH1 cells to regulate flexibility with a TFH-like gene profile. Nat. Immunol. *13*, 405–411.

Oxenius, A., Bachmann, M.F., Zinkernagel, R.M., and Hengartner, H. (1998). Virus-specific MHC-class II-restricted TCR-transgenic mice: effects on humoral and cellular immune responses after viral infection. Eur. J. Immunol. *28*, 390–400.

Parish, C.R., and Liew, F.Y. (1972). Immune response to chemically modified flagellin. 3. Enhanced cell-mediated immunity during high and low zone antibody tolerance to flagellin. J. Exp. Med. *135*, 298–311.

Pepper, M., and Jenkins, M.K. (2011). Origins of CD4(+) effector and central memory T cells. Nat. Immunol. *12*, 467–471.

Pepper, M., Pagán, A.J., Igyártó, B.Z., Taylor, J.J., and Jenkins, M.K. (2011). Opposing signals from the Bcl6 transcription factor and the interleukin-2 receptor generate T helper 1 central and effector memory cells. Immunity *35*, 583–595.

Portnoy, D.A., Auerbuch, V., and Glomski, I.J. (2002). The cell biology of Listeria monocytogenes infection: the intersection of bacterial pathogenesis and cell-mediated immunity. J. Cell Biol. *158*, 409–414.

Rees, W., Bender, J., Teague, T.K., Kedl, R.M., Crawford, F., Marrack, P., and Kappler, J. (1999). An inverse relationship between T cell receptor affinity and antigen dose during CD4(+) T cell responses in vivo and in vitro. Proc. Natl. Acad. Sci. USA *96*, 9781–9786.

Rudensky, A.Y., Preston-Hurlburt, P., Hong, S.C., Barlow, A., and Janeway, C.A., Jr. (1991). Sequence analysis of peptides bound to MHC class II molecules. Nature *353*, 622–627.

Smith-Garvin, J.E., Koretzky, G.A., and Jordan, M.S. (2009). T cell activation. Annu. Rev. Immunol. *27*, 591–619.

Speiser, D.E., Baumgaertner, P., Voelter, V., Devevre, E., Barbey, C., Rufer, N., and Romero, P. (2008). Unmodified self antigen triggers human CD8 T cells with stronger tumor reactivity than altered antigen. Proc. Natl. Acad. Sci. USA *105*, 3849–3854.

Stemberger, C., Huster, K.M., Koffler, M., Anderl, F., Schiemann, M., Wagner, H., and Busch, D.H. (2007). A single naive CD8+ T cell precursor can develop into diverse effector and memory subsets. Immunity *27*, 985–997.

Stetson, D.B., Mohrs, M., Mallet-Designe, V., Teyton, L., and Locksley, R.M. (2002). Rapid expansion and IL-4 expression by Leishmania-specific naive helper T cells in vivo. Immunity *17*, 191–200.

Taswell, C. (1981). Limiting dilution assays for the determination of immunocompetent cell frequencies. I. Data analysis. J. Immunol. *126*, 1614–1619.

Utz, U., Biddison, W.E., McFarland, H.F., McFarlin, D.E., Flerlage, M., and Martin, R. (1993). Skewed T-cell receptor repertoire in genetically identical twins correlates with multiple sclerosis. Nature *364*, 243–247.

Vanguri, V., Govern, C.C., Smith, R., and Huseby, E.S. (2013). Viral antigen density and confinement time regulate the reactivity pattern of CD4 T-cell responses to vaccinia virus infection. Proc. Natl. Acad. Sci. USA *110*, 288–293.

Yamane, H., Zhu, J., and Paul, W.E. (2005). Independent roles for IL-2 and GATA-3 in stimulating naive CD4+ T cells to generate a Th2-inducing cytokine environment. J. Exp. Med. *202*, 793–804.

Yu, D., Rao, S., Tsai, L.M., Lee, S.K., He, Y., Sutcliffe, E.L., Srivastava, M., Linterman, M., Zheng, L., Simpson, N., et al. (2009). The transcriptional repressor Bcl-6 directs T follicular helper cell lineage commitment. Immunity *31*, 457–468.

Zhu, J., Yamane, H., and Paul, W.E. (2010). Differentiation of effector CD4 T cell populations (*). Annu. Rev. Immunol. *28*, 445–489.